CMS Conference Report

29 August 2007

The simulation of the CMS electromagnetic calorimeter

F. Cossutti

Istituto Nazionale di Fisica Nucleare - Sezione di Trieste, Trieste, Italy

on behalf of the CMS ECAL Group

Abstract

The CMS Collaboration has developed a detailed simulation of the electromagnetic calorimeter (ECAL), which has been fully integrated in the collaboration software framework CMSSW. The simulation is based on the Geant4 detector simulation toolkit for the modelling of the passage of particles through matter and magnetic field. The geometrical description of the detector is being re-implemented using the DetectorDescription language, combining an XML based description with the algorithmic definition of the position of the elements. The ECAL simulation software is fully operational and has been validated using real data from the ECAL test beam experiment that took place in summer 2006.

Poster presented at *CHEP 2007*, Victoria, BC (Canada), September 5, 2007

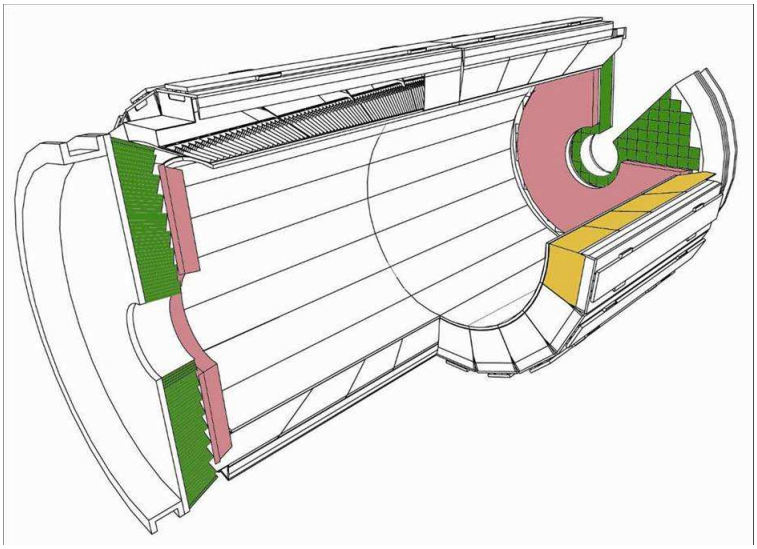

Figure 1: View of the ECAL structure.

1 Introduction

The CMS Collaboration [1] has started in 2005 to re-implement its simulation, reconstruction and analysis software in a new framework, called CMSSW. The simulation of the electromagnetic calorimeter of CMS (ECAL) [2] has been ported into this new framework, and this porting has been the opportunity for a revision of several parts of it.

Moreover, during the year 2006 an intense test beam campaign has involved ECAL, alone and in a combined test with the hadronic calorimeter (HCAL). The simulation of the test beam setups has been developed in the new framework, fully integrated with the official one. This allows the validation and tuning of the final version of the ECAL simulation directly on the test beam data.

2 The ECAL layout

CMS is a general purpose detector which will operate on the LHC (Large Hadron Collider) at CERN. LHC will deliver proton-proton collisions at a centre-of-mass energy of 14 TeV, with a design luminosity of $10^{34}\text{cm}^{-2}\text{s}^{-1}$. The crossing rate will be of 40 MHz and up to 20 events with 1000 tracks will be produced on average per bunch crossing at the highest luminosity.

One of the key issues at LHC is the search for the Higgs boson. The golden channel to discover a Higgs with mass between 100 and 150 GeV/c^2 is the decay $H \rightarrow \gamma\gamma$. The requirement imposed by LHC and by the reconstruction of this channel have been the benchmarks to define the electromagnetic calorimeter characteristics, which will be placed between the tracker and the hadronic calorimeter, inside the 4 Tesla solenoidal magnetic field of CMS.

The ECAL structure is shown in fig. 1. Lead tungstate ($PbWO_4$) crystals have been chosen by CMS for ECAL, because of their excellent energy resolution. Thanks to the high density (8.28 g/cm^3) and the small radiation length (0.89 cm) of $PbWO_4$, the calorimeter is very compact and can be placed inside the magnetic coil needed for the tracker. The small value of the Molière radius (2.2 cm), well matches the very fine granularity needed by the high particle density of the events at LHC. The fast scintillation mechanism (80% of the light is emitted within 25 ns, i.e. one bunch crossing length) allows the crystals to be used at the LHC crossing rate of 40 MHz. The drawbacks of $PbWO_4$ are the low light yield (100 photons/MeV) which imposes a multiplication mechanism in the photodetector, and the strong temperature dependence on the crystal response (1/L.Y dL.Y./dT $\simeq$ -1.9%/°C), which imposes stringent requirements on the cooling system.

The ECAL structure is made by a barrel, covering the central rapidity region ($|\eta| < 1.48$) and two endcaps, which extend the coverage up to $|\eta| < 3$. In the barrel 61200 crystals with a tapered shape are positioned at a radius of 1.29 m, with a transverse granularity of $\Delta\eta \times \Delta\phi = 0.0175 \times 0.0175$, and a radiation length of 25.8 X_0. The crystals are organized in 36 super-modules, 18 for each half, each with a total number of 1700 crystals. In the endcap, 14648 crystals with a lenght of 24.7 X_0 and a transverse granularity $\Delta\eta \times \Delta\phi$ ranging from 0.0175×0.0175 to 0.05×0.05 are positioned at a distance of 3.17 m from the interaction point. They are organized into 2 D-shaped regions (Dees) for each side. Tilts of 3° both in η and ϕ give the structure a geometry slightly off-pointing from

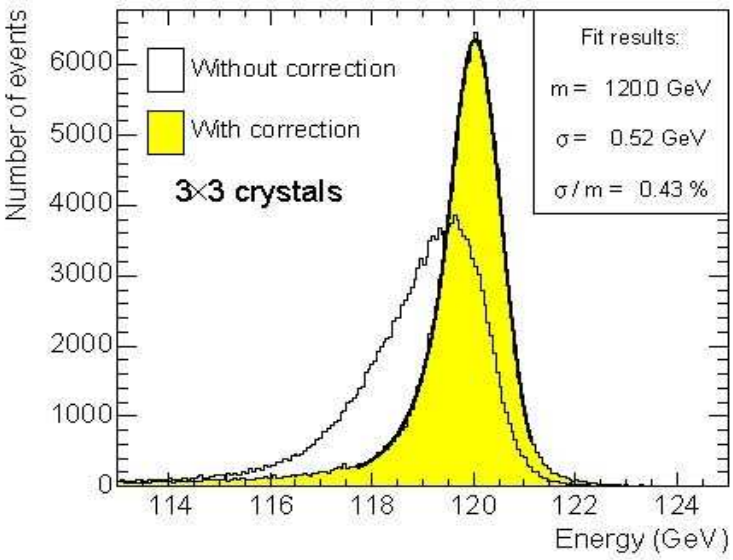

Figure 2: Distribution of energy before (unshaded) and after cluster containment corrections (shaded) for a 3×3 crystals matrix.

the interaction region, in order to improve the hermeticity of the detector.

In the barrel the scintillation light is read by Avalanche Photo-Diodes (APD), while in the endcap Vacuum Photo-Triodes (VPT) are used.

In front of the endcap, in order to improve the separation between electrons and π^0, a Si-Pb preshower is installed, for a global depth of 3 X_0. The readout is made by 137729 silicon strips ($\simeq 63 \times 1.9\,\mathrm{mm}^2$) organized in two planes for each side.

3 ECAL performances and simulation

The Higgs mass resolution in the $H \rightarrow \gamma\gamma$ channel depends linearly on the photon energy resolution achieved. This leads to challenging requirements on the ECAL energy resolution. The results achieved in the 2004 test beam are [3]:

$$\frac{\sigma_E}{E} = \frac{2.8\%}{\sqrt{E}} \otimes \frac{0.125}{E} \otimes 0.3\% \quad \text{(E in GeV)} \tag{1}$$

where the three terms on the right hand side of the expression represent, respectively, the stochastic, noise and constant term. The main effects contributing to these terms are:

- for the stochastic term, the limiting factor is the photo-electron statistics, and the lateral shower fluctuations are also contributing;
- noise is basically due to the electronics noise, and in the CMS data taking the effects of the pileup will also influence this term;
- the constant term gets contributions form the light yield non uniformity, in CMS from the limited knowledge of the inter-calibration, and from the rear energy leakage.

The result shown is obtained summing all the energies measured by a matrix 3×3 of crystals centered around the crystal at which the beam is pointing. This result is obtained for a central impact of the particles on the crystal, defined as an area of $4 \times 4\,\mathrm{mm}^2$ around the maximum shower contaninment point [3]. As discussed in this reference, the energy resolution is strongly dependent on the impact position of the incident particle, and in order to optimize it it is necessary to evaluate a position dependent cluster containment correction.

In figure 2 the distribution of the measured energy before and after cluster containment corrections for a 3×3 crystals matrix is presented. As described in [3], the cluster containment corrections can be determined from test beam data exploting the pure energy measurements of the crystals, avoiding the need for position measurements

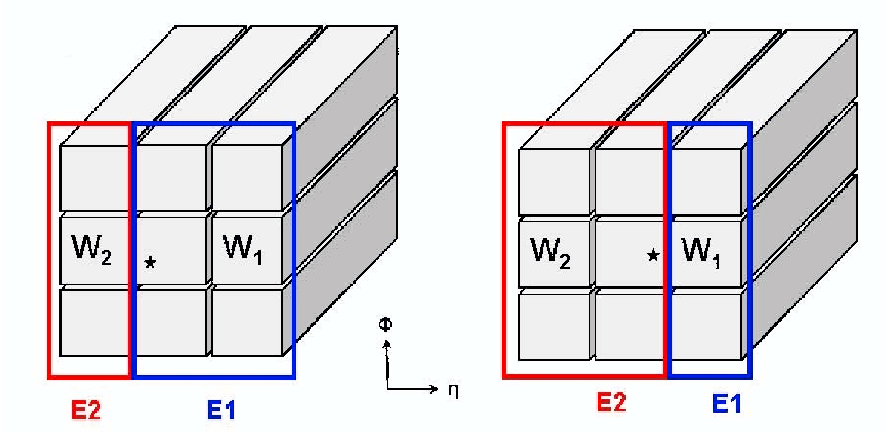

Figure 3: Containment corrections as a function of η: definition of E_1 and E_2 in the case where $W_1 < W_2$ (left) and $W_1 > W_2$ (right). The star represents the position of impact of an electron, W_1 and W_2 the energies measured in single crystals on the high and low η sides of the central crystal.

which are not possible for photons. The correction in η is determined as a function of the observable $\ln E_1/E_2$, where the energies E_1 and E_2 are measured as shown in figure 3. The correction as a function of ϕ is determined in the same way, but partitioning the crystal matrix energy along this coordinate instead of η as previously done.

This measurement is obviously sensitive to the transverse development of the shower, and is anyway done in absence of magnetic field, which is known to influence the transverse development. The link between the test beam environment and the CMS one for this particular aspect is given by the simulation. It is therefore very important to tune it at best on the test beam data, especially as far as the transverse shape of the shower is concerned, in order to rely on it to determine the corrections inside the magnetic field.

4 Description of the ECAL simulation

In 2005 the CMS Collaboration started the effort to move all its software into a new single framework, named CMSSW, and all the functionalities of the previous software components were integrated into it. Concerning the ECAL simulation, this re-implementation has been also the opportunity to re-implement significant portions of the code, in particular the detector description and the digitization model.

Furthermore, a major goal of the 2006 test beam campaign has been to move all the test beam related code into the official CMSSW framework, in order to be able to fine tune directly the same setup which will be then used for the CMS simulation.

The ECAL simulation is composed of 3 main parts: the description of the detector, the tracking of particles produced by an event generator in the magnetic field through the detector itself, and the model which describes the output of the electronic readout of the detector.

4.1 Detector description

The description of the detector involves the description of the geometrical properties of its components, of their relationships, of their relative positions, and of the characteristics of the materials which they are made of. This description is needed by different software tasks: simulation, reconstruction, visualization. The approach adopted in CMS has been to unify the description under a single architecture, named Detector Description Database (DDD) [5].

This package allows the represention of the detector as an acyclic multigraph structure in which the description is compactified. This structure can be translated into an expanded view, corresponding to a tree structure of volumes contained into other higher level ones. The package uses XML as language to encode the description itself through the Detector Description Language schema, although the whole architecture is independent on the actual language used for the practical implementation.

XML instructions are used to describe the constants needed to specify the geometry, both as positions and volumes characteristics, besides the material properties.

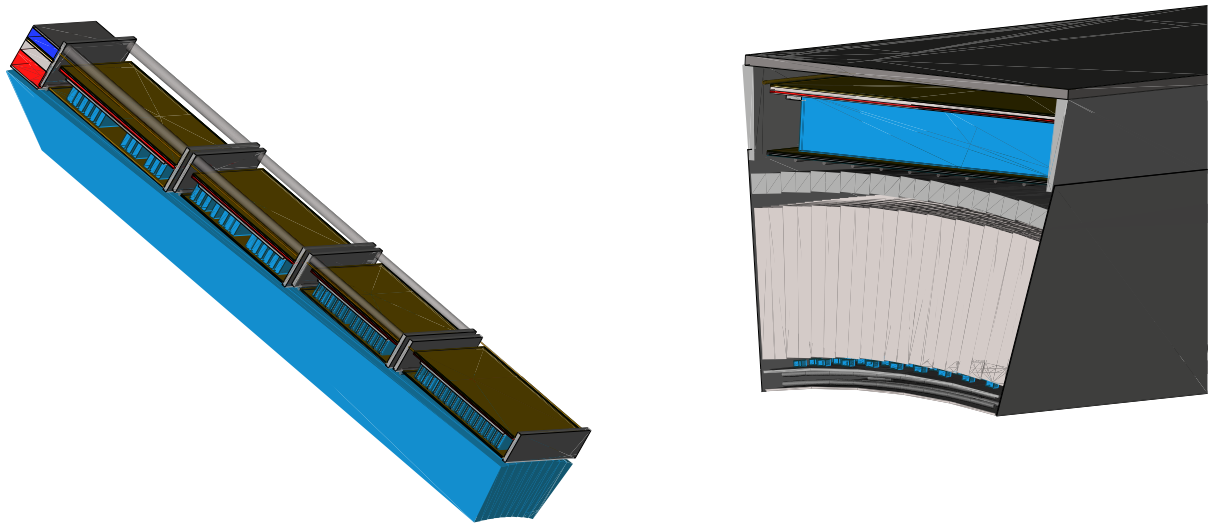

Figure 4: View of the geometrical description of an ECAL barrel supermodule as obtained after the update according to the most recent engineering drawings. On the left: supermodule with the details of the structure behind the crystals shown. On the right: transverse view of a supermodule.

The actual specification of the volumes and of the position of each of their copies is performed, possibly exploiting the symmetries in the structure, in a C++ code which gets the parameters from the XML file as input. In this way the size of the XML description is significantly reduced from about 50k lines to a few thousands of lines, allowing for a more flexible implementation, easier to maintain and modify if needed.

The actual description has been based onto the latest drawings of the detector, especially as far as the passive materials (cooling, electronics boards, cables) are concerned, relevant as material in front of the hadronic calorimeter. The material budget in the description has been verified and tuned using the measurements of the weights of the different components done in the laboratory. A view of the barrel supermodule updated description can be seen in figure 4. The possibility to compare data taken in the combined ECAL/HCAL test beam with the simulation can allow the understanding of the reliability of the description of the material in front of the hadronic calorimeter.

4.2 Model of particle passage through matter and magnetic field

The tracking of the initial particles, produced by some event generator, through the solenoidal magnetic field, and the description of their interaction with the detector matter are done using Geant4 [4] as a backbone. At present the version 4.8.2p01 is used with QGSP_EMV physics list. Next versions and other physics lists are currently under scrutiny.

The CMS specific code has the main purpose to model the sensitive detectors specific behaviour and to produce the persistent objects which will be stored in the simulation output. In the ECAL simulation the crystals and the preshower silicon strips are considered as sensitive devices. The specification that a given volume has to be considered as sensitive by the simulation is done again in the XML based description through a special block of information, for instance:

```
<SpecParSection label="ecal" eval="true">
   <SpecPar name="ecal_eb">
   <PartSelector path="//EBRY.*"/>
   <Parameter name="SensitiveDetector"
   value="EcalSensitiveDetector"
   eval="false"/>
   <Parameter name="ReadOutName"
   value="EcalHitsEB" eval="false" />
   <Parameter name="nxtalEta"
```

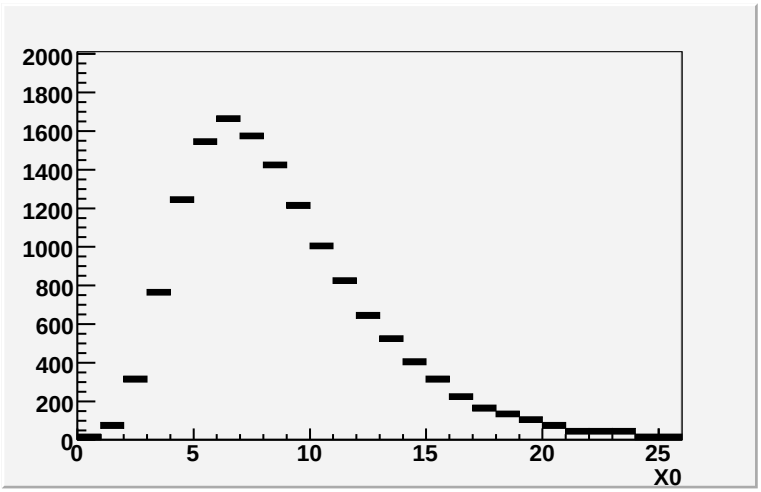

Figure 5: Simulated longitudinal profile of the energy deposit in a crystal for a 30 GeV electron with central incidence. The depth is measured in radiation legths X_0

.

```
   value="85.0"/>
   <Parameter name="PhiBaskets"
   value="18.0"/>
   <Parameter name="nxtalPhi"
   value="360.0"/>
   <Parameter name="EtaBaskets"
   value="25.0"/>
   <Parameter name="EtaBaskets"
   value="45.0"/>
   <Parameter name="EtaBaskets"
   value="65.0"/>
   <Parameter name="EtaBaskets"
   value="85.0"/>
 </SpecPar>
```

The persistent object stored in memory as output of the ECAL simulation is the `CaloHit`. This object contanins a number of identifiers which uniquely tag the sensitive volume in which it has been produced, the Geant4 track entering in the main ECAL volume that has subsequently produced it in its shower, and the event identified (for pileup simulation). Then it contains the energy deposit, as sum of all the deposits integrated over one nanosecond, and the time of the deposit with respect to the event generation (i.e. the bunch crossing) moment.

The production cuts adopted for electrons, positrons and photons are 1 mm in the crystals, and 0.1 mm in the silicon strips.

4.3 Model of sensitive detector response

The ECAL simulation simplifies the description of the physics processes chain that happens following an energy deposit by a particle in the crystal volume. There is no attempt to simulate the emission of scintillation light, its optical propagation in the detector, accounting for absorption, and the explicit behaviour of APD or VPT sensitive devices, both as geometric acceptance and quantum efficiency. All these processes are condensed in an effective conversion between the `CaloHit` energy deposit and the average number of photo-electrons produced in the devices, according to the measurements in laboratory.

The main purpose of this conversion is to correctly simulate the Poisson photo-statistics fluctuation happening in the conversion process, which is the main contribution to the stochastic term in the energy resolution. The conversion factors used (2.25/1.8 photo-electrons/MeV for barrel/endcap respectively) already account for the additional excess noise factor due to the fluctuations in the avalanche process in the sensitive devices.

Another physical process which is described in a simplified way is the non uniformity in the longitudinal light yield. For the front part of the crystal, corresponding to the first half of the longitudinal profile of the shape (see

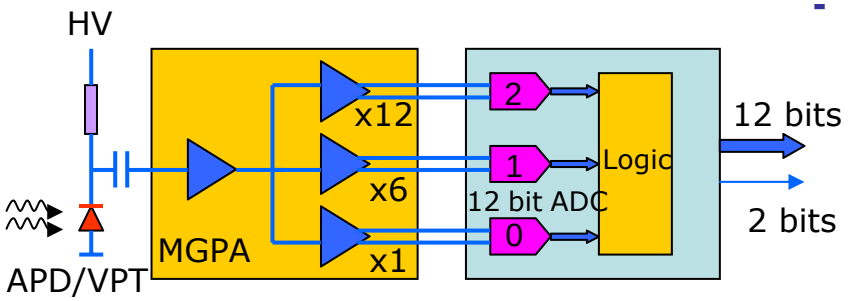

Figure 6: Schematic view of the signal processing chain as implemented in the ECAL readout electronics.

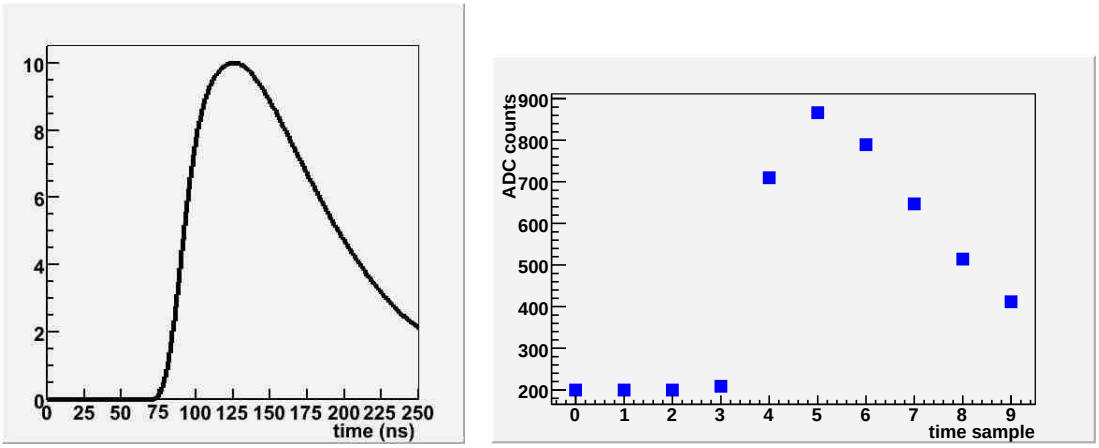

Figure 7: On the left: MGPA signal shape implemented in the simulation of the electronic readout. On the right: ECAL crystal readout output signal made by 10 time ordered samples of ADC output, corresponding to the digitzation of the shape shown on the left.

figure 5) this non uniformity is measured to be compatible with zero. The uncertainty on this value is effectively accounted for as a constant smearing to the energy deposit with an rms of 0.3%. For the rear part of the crystal, where only the tail of the shower falls, the non uniformity is slowly varying up to 2%, and this is effectively described by reweighting the energy deposit in this part of the crystal by a factor varying linearly between 1 and 1.02.

4.4 Model of electronics response

The last step in the ECAL simulation is the model of the electronics response, which produces as persistent object the same digitization output coming from the real detector, the `EcalDataFrame`. The actual output of each subdetector is a derived object from this base one.

A simple scheme of the crystals readout electronics is shown in figure 6. A Multi Gain Preamplifier (MGPA), processes the signal coming from the APD/VPT devices with three possible gains ($\times 1$, $\times 6$ and $\times 12$). The measured shape of the MGPA is implemented in the code, see the left side plot of figure 7. Each of these signals is digitized by a 40 MHz multi-channel ADC, which encodes the signal output in 12 bits, plus 2 bits for the gain identification. The highest gain corresponding to a non saturated signal is finally chosen.

The persistent output is a time ordered set of 10 samples corresponding to 10 ADC clock ticks, see the right side plot of figure 7. The timing is adjusted in such a way that the MGPA signal maximum is sampled on the 6th clock tick. For gain 12, the first three samples are used to measure directly the pedestal of the signal.

The output is easier for the preshower, where only 3 time samples and one gain are used.

In the re-implementation of this model in CMSSW, great care has been put in refining the description of all the details of the electronics, compared to the previous situation. The gain switch mechanism, with the proper saturation and gain hysteresis are now fully implemented. The pedestal is added, and particular attention has been

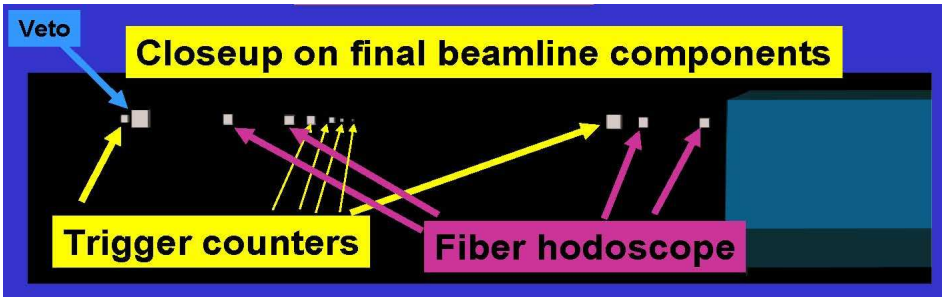

Figure 8: Close view of the details of the H4 beam line as described in the test beam simulation.

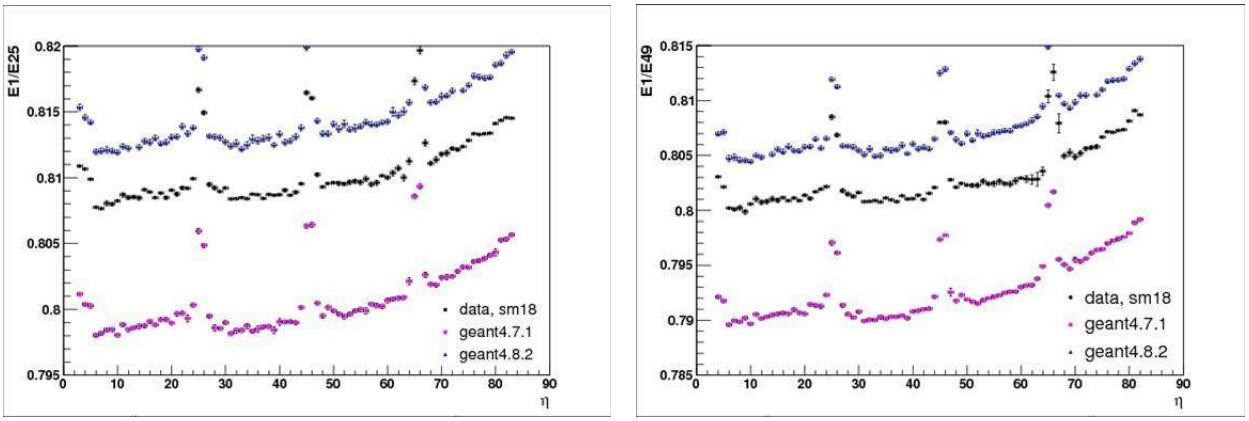

Figure 9: On the left: distribution of the ratio E_1/E_{25} as a function of η, e.g. the crystal position in the supermodule. On the right: the same distribution for E_1/E_{49}. The central curve represent real data, the lower one the simulation using Geant 4.7.1, the upper one the simulation based on Geant 4.8.2.

put in reproducing exactly the measured noise of the electronics. The possibility to have correlation between noise in the different time samples is foreseen, although still under study.

A detailed simulation of the digitization step is important in the CMS frame to correctly account for the pileup description.

After this step, the signal is sent to the code that deterministically emulates the trigger primitives calculation and their use for the Selective Readout mechanism for crystals, as well as the zero suppression for the preshower [6].

5 Validation on test beam data

The validation of all the components of the simulation of ECAL is ongoing, using the data collected during the 2006 test beam campaign performed in the CERN north area. Data collected in the H4 line with one fully equipped barrel supermodule exposed to electron beams are used to validate the description of electromagnetic showers. The data taken at the H2 line, where a combined ECAL+HCAL test was performed with hadronic beams, are important to understand the repsonse to early hadronic showers and the combined calorimetry.

The test beam simulation includes the description of the beam lines, in order to describe the material in front of the modules to be tested and the sensitive devices used to monitor the beam position. Figure 8 shows the detail of the scintillators telescope and of the hodoscopes of the H4 line used to monitor the beam acceptance and position. This line is described down to the last present magnet.

As discussed in section 3, the simulation validation on the test beam is primarily focussed on the transverse shape of the electromagnetic showers. The observables sensitive to it which are studied are the ratios between the energy deposited in the central crystal of the shower (E_1) over the energy collected in a matrix of crystals of given size (3×3, 5×5, 7×7) centered on the central crystal. Figure 9 shows the distribution of E_1/E_{25} and E_1/E_{49} as measured on the test beam, compared with the simulation predictions, using both Geant4.7.1 and Geant4.8.2. The behavior as a function of η is very well described. The absolute value of the ratio agrees within 1% with the real

data, and shows variations with the Geant4 versions. The reason for these changes appears to be linked to the multiple scattering treatment, which has slightly changed between the two versions. Studies are still ongoing to fully complete the simulation validation.

6 Conclusion

The simulation of the CMS electromagnetic calorimeter has been ported to the new CMSSW software framework, and several of its components have been improved.

The use of this software for the analysis of the 2006 test beam data will allow the validation both the detector description and the physics model on real data before the start of the CMS data taking, allowing a detailed scrutiny of the code and the best tuning to optimize its performances.

Acknowledgment

The author would like to thank the CMS Collaboration members that have reviewed the material presented in this work.

References

[1] The CMS Collaboration, "The Compact Muon Solenoid Technical Proposal", CERN/LHCC 94/38, LHCC/P1 (1994).

[2] The CMS Collaboration, "The Electromagnetic Calorimeter Technical Design Report", CERN/LHCC 97-33, CMS TDR 4 (1997).

[3] P. Adzic *et al.*, "Energy Resolution of the Barrel of the CMS Electromagnetic Calorimeter", J. Instrum. 2 P04004 (2007)

[4] S. Agostinelli *et al.*, NIM **A** 506 (2003) 250;
J. Allison *et al.*, IEEE Transaction on Nuclear Science **53** N. 1 (2006) 270.

[5] M. Liendl *et al.*, "The Role of XML In The CMS Detector Description Database", CMS CR 2001/008, presented at CHEP01 Computing on High Energy Physics and Nuclear Physics, Beijing, Sep. 3-7, 2001;
M. Case *et al.*, "Detector Description Domain Architecture and Data Model", CMS Note 2001/057 (2001).

[6] The CMS Collaboration, "CMS Physics Technical Design Report - Volume I: Detector Performance and Software", CERN/LHCC 2006-001, CMS TDR 8.1 (2006).